coatings

MDPI

Article

The Tribological Behavior of TiN/TiC CVD Coatings under Dry Sliding Conditions against Zirconia and Steel Counterparts

Miklós Jakab [1,*], Osamah Ihsan Ali [2], István Gábor Gyurika [2], Tamás Korim [1] and Judit Telegdi [3,4]

[1] Department of Materials Engineering, Research Centre for Engineering Sciences, University of Pannonia, Egyetem St. 10, H-8210 Veszprém, Hungary; korim.tamas@mk.uni-pannon.hu
[2] Department of Mechanics, Research Centre for Engineering Sciences, University of Pannonia, Egyetem St. 10, H-8210 Veszprém, Hungary; osamah.ihsan.ali@phd.uni-pannon.hu (O.I.A.); gyurika.istvan.gabor@mk.uni-pannon.hu (I.G.G.)
[3] Research Centre for Natural Sciences, ELKH, Magyar Tudosok Krt. 2., H-1117 Budapest, Hungary; telegdi.judit@ttk.hu
[4] PhD School of Material Sciences and Technologies, Óbuda University, Doberdó u. 6., H-1034 Budapest, Hungary
* Correspondence: jakab.miklos@mk.uni-pannon.hu

Abstract: During this research work, the wear and friction properties of TiN/TiC coatings produced with different manufacturing parameters were investigated against steel and zirconium counterparts. The coatings, which were deposited on WC–Co substrate, were characterized based on their microstructure, phase composition, and microhardness. The tribological behavior of the coatings was examined in accordance with ASTM G99 and ASTM G133 standards using pin-on-disc tests with steel and zirconium counterfaces, while the adhesion of the coatings was investigated with a modified scratch test. According to the results obtained from the experiments, the use of zirconium counterpart is advantageous even for coatings produced with different microhardness and layer thickness using the CVD method. The results show that the change in the friction coefficient can be well traced with properly chosen parameters, thereby determining the wear resistance of the coating.

Keywords: CVD; TiN; TiC; tribological behavior; wear-resistant coatings; zirconia

check for updates

Citation: Jakab, M.; Ali, O.I.; Gyurika, I.G.; Korim, T.; Telegdi, J. The Tribological Behavior of TiN/TiC CVD Coatings under Dry Sliding Conditions against Zirconia and Steel Counterparts. *Coatings* **2023**, *13*, 832. https://doi.org/10.3390/coatings13050832

Academic Editor: Esteban Broitman

Received: 11 April 2023
Revised: 21 April 2023
Accepted: 21 April 2023
Published: 26 April 2023

Copyright: © 2023 by the authors. Licensee MDPI, Basel, Switzerland. This article is an open access article distributed under the terms and conditions of the Creative Commons Attribution (CC BY) license (https://creativecommons.org/licenses/by/4.0/).

1. Introduction

Chemical vapor deposition (CVD) can be defined as deposition of a solid onto a heated surface caused by a vapor-phase chemical process. It belongs to the atomistic class of vapor-transfer processes, which means that the deposition species are atoms, molecules, or a combination of both [1–3]. Therefore, CVD is a technology that relies on the production of a gaseous species carrying the coating material within a coating reactor or chamber. Alternatively, the gaseous species could be created outside of the coating reactor and delivered through a delivery system. These gaseous species can come into direct contact with the surface that needs to be coated. The reactor is kept at a high temperature, which can reach up to 2000 °C [4,5]. The CVD process can be used to create a wide range of coatings, from soft, ductile coatings to those with hard, ceramic-like characteristics. Coatings can have a hardness ranging from 150 to 3000 HV (0.1 kgf). Currently, CVD coatings are being utilized to prevent the severe attrition of components used in various industrial situations where corrosion, oxidation, or wear occurs [4,6,7].

Generally, TiN and TiC coatings have been used on cutting tools for over three decades and continue to be important components of current tools. Titanium nitride and titanium carbide (TiN, TiC) are well-known for their strong adhesion, high melting point, chemical stability, lack of phase change, high hardness, and wear resistance. The use of TiN and TiC improves the thermal stability, oxidation behavior, and abrasive wear of the coating [8,9]. Consequently, applying TiN and TiC coatings on cutting tool materials increases features

such as hot hardness, thermal shock, oxidation, chemical stability, toughness, and tribological characteristics [10].

So, Ti (C, N) is commonly used as a protective coating in the metal-cutting industry because of the combination of tough TiN and hard TiC characteristics [11,12]. Numerous studies [13–16] have shown that Ti (C, N) coatings exhibit low surface roughness and high hardness due to their fine-crystallized surface. Based on previous studies, the hardness of TiC- and TiN-based coatings produced by different methods (PACVD, PVD, and self-propagating high-temperature synthesis (SHS)) is approximately 30 GPa, while their elastic modulus is around 230 GPa. The temperature applied during the production of the samples was below 1000 °C in all cases. Tribological characteristics are crucial for evaluating the performance of cutting tools, and multiple studies have shown that Ti (C, N) coatings exhibit a lower wear rate. Ti (C, N)-coated tools have been reported to last twice as long as uncoated tools [17–21].

It is worth mentioning that TiN belongs to the interstitial compound group and crystallizes in the fcc B1-NaCl structure. TiN is stable throughout a wide composition range. Bulk materials have been observed with nitrogen to titanium ratios ranging from 0.6 to 1.16. Under-stoichiometric films (N/Ti < 1.0) have vacancies on the N-sublattice, while over-stoichiometric films (N/Ti > 1.0) have vacancies on the Ti-sublattice. TiC has almost the same crystal structure as TiN (B1-NaCl), but due to stronger covalent bonding, it has a higher hardness. Miscibility can occur between TiN and TiC, where nitrogen in the fcc structure can be freely replaced by carbon, forming a TiCxN1-x ($0 \leq x \leq 1$) solid solution. The steady variation in composition allows for the regular adjustment of coating properties [22].

The strong mechanical properties of TiN make it highly effective for use in a variety of applications. Additionally, TiN's attractive golden color allows for wear detection and serves as a marketing argument. Thermal CVD deposition of TiN on cemented carbide tools, in particular, is a well-established procedure using the precursors $TiCl_4$, N_2, and H_2. $TiCl_4$ and N_2 provide the elements which constitute the coatings, while H_2 acts as a reduction agent. Argon is used as a carrier gas and to produce a total flow rate high enough to achieve the required mass fluxes and deposition rates. These films are typically stoichiometric, with minor chlorine incorporations. The coatings have a columnar microstructure and excellent adherence to cemented carbide [23,24]. The application of surface coatings allows for the production of components with specific tribological properties, such as low coefficients of friction, high wear resistance, or both. While the surface coating provides tribological functions, the bulk material can be selected based on characteristics such as stiffness, strength, or cost. Therefore, coating tools and machine components is a highly effective technique for increasing the lifetime and productivity of parts [25–27].

The tribological behavior of materials has been studied by many researchers using a variety of techniques, including ball-on-disc, ball-cratering, fretting, rubber-wheel abrasion, etc. A crucial factor to consider when choosing a tribological model test is the type of stresses that the investigated material systems will experience in industrial use. The aim of the present study is to investigate TiN/TiC-based coatings with steel and zirconium static counterparts. When low surface roughness of ceramic products is critical, such as in high-pressure pistons, selecting the right tool for precise size grinding is important. In such cases, the specimen is subjected to linearly alternating kinetic stresses during use and machining, which are best modeled using a pin-on-disc tribometer [28–30]. A ball-on-disc approach has been used by numerous authors to explore the wear behavior and wear rate of TiN and TiC coatings. Among them, researchers investigated the effect of sliding speed on the wear rate of TiN and TiC coatings at different linear speeds ranging from 5 to 30 cm/s (sometimes reaching up to 200 cm/s) against an Al_2O_3 ceramic ball and steel ball at different loads from 2.5 N up to 25 N, comparing the effects of the TiN and TiC coating layers on the wear performance of the cermet (which is used as a cutting tool insert). The cermet is a composite material made from ceramic and metal that can combine beneficial characteristics of both metals and ceramics, such as the capacity for plastic deformation

and high temperature resistance and hardness. A carbide or oxide, such as WC, is bound to the metal with nickel, molybdenum, and cobalt typically being the metals used [31–34].

Moreover, researchers investigated the wear behavior of TiN and TiC coatings at high sliding speeds of about 200 cm/s with a normal load of 10 N and sliding distance up to 678 m against an SiC ball. They also tested the wear behavior of TiN (N-rich) and TiC (C-rich) coatings with a sliding speed of 20 cm/s, a normal load of 2.5 N, and a sliding distance of about 1000 m, using a traditional ball-on-disc tribometer to compare the tribological behaviors of TiN and TiC coatings against steel and alumina balls at two distinct contact loads of about 1 N to 5 N, and three different sliding speeds of 0.1, 0.3, and 0.5 m/s.

Although the CVD deposition of TiN and TiC is widely known, most studies focus on the growth of the coatings, mechanical characteristics, or tribological behavior. However, only a few consider the investigation of the tribological behavior of the coatings against different materials and investigate the effects of these results on the coating morphology and the resultant mechanical properties [35–38].

Typically, sliding tests to determine the wear rate, wear behavior, and coefficient of friction of TiN and TiC coatings are generally performed using balls made of alumina or steel. However, there are no investigation studies on the wear behavior of the coatings using a zirconia (ZrO_2) ball.

The goal of this study is to investigate the tribological properties of two-layer coatings (TiC and TiN) created with various manufacturing parameters. Both sample preparations used WC–Co cermet as the substrate. To compare the wear mechanisms, steel and zirconia counterparts were used. The tests aimed to demonstrate that, in many cases, zirconia is preferred over steel due to its higher hardness and better wear resistance. Studying the wear and friction properties of zirconium is crucial for the ceramic industry, especially in areas that require precise fit and low surface roughness, such as medical applications, pistons, and grinding equipment.

2. Materials and Methods

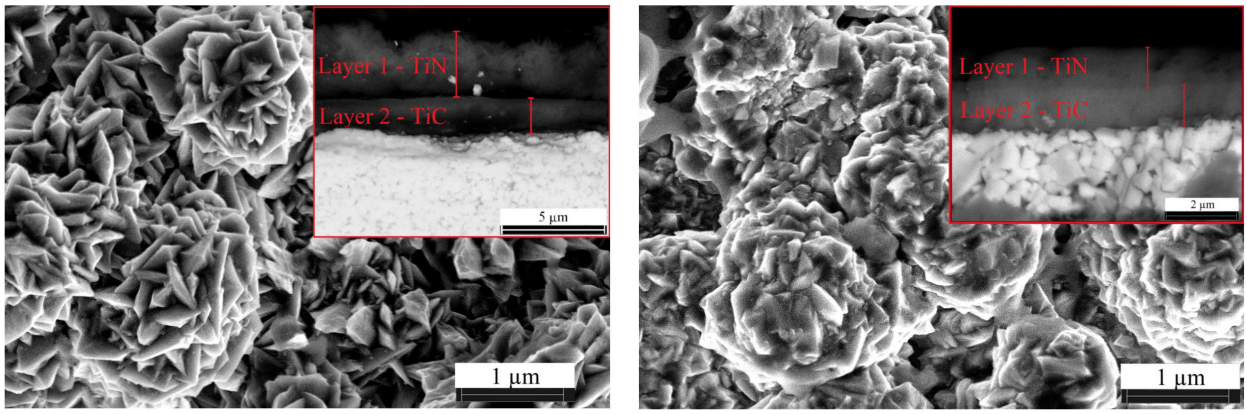
2.1. Materials

The coatings have been produced by thermal CVD in an industrial reactor (Büttner Ltd., Nagyatád, Hungary) using the manufacturing parameters shown in Table 1. The process was performed using the precursors titanium–tetrachloride ($TiCl_4$), nitrogen (N_2), hydrogen (H_2) and argon (Ar), where WC–Co cermet (Voestalpine Eifeler GmbH, Düsseldorf, Germany) was used as a substrate. In the case of Sample A, a lower temperature and twice the pressure was applied compared to Sample B. The precursor gas flow rate (Standard Liters per Minute—SLM) was kept at nearly the same value, and the TiC layer was produced under identical conditions for both samples.

Table 1. The manufacturing parameters for preparation of the samples used in present study.

Sample	Layers	Time (h)	Temperature (°C)	Pressure (mbar)	SLM H_2	SLM CH_4	SLM N_2	SLM TCl_4
A	TiN	3.0	980	100	4.10		4.1	8.20
	TiC	2.0	1000	80	9.24	1.0		8.22
B	TiN	3.0	1020	50	3.50		4.5	8.00
	TiC	2.0	1000	80	9.24	1.0		8.22

The microstructure of the coatings formed on identical substrates is shown in Figure 1. The red-marked image shows the backscattered electron images taken from the cross-sectional polished samples, where the layer thickness was measured. On the surface of Sample A (Figure 1a), TiN is present in a more crystallized form, while Sample B (Figure 1b) typically shows rounded shapes. The sharp crystals seen in Sample A may play an important role in terms of tribology, as they can remove material from the surface of the counterpart to a much greater extent.



(**a**) (**b**)

Figure 1. Surface morphology and cross-sectional images of the coated samples: (**a**) Sample A; (**b**) Sample B.

The thicknesses of the different layers are summarized in Table 2. The values presented in the table represent the results of 5 parallel measurements. In both samples, the thickness of the TiC layer formed is nearly the same, but in the case of Sample A, the thickness of the top layer is twice as much as that of Sample B. Presumably, the applied pressure value is the reason why many sharp crystals are present on the surface, in greater thickness.

Table 2. Coating thickness of the samples.

Layers Thickness (µm)	TiC	TiN	Total
A	1.6 ± 0.1	3.2 ± 0.3	4.8 ± 0.3
B	1.3 ± 0.1	1.6 ± 0.1	2.9 ± 0.2

The elemental composition of the different coatings is summarized in Table 3. The measurements were performed on cross-sectional samples. The composition of the titanium-based coatings is nearly stoichiometric, with the Ti:C and Ti:N ratios being approximately 1:1 in each case.

Table 3. The elemental composition (At. %) of the substrate and the CVD-coated samples.

Sample		Ti	N	C	W	Co
Substrate		-	-	-	78.0 ± 2.7	22.0 ± 1.3
A	Layer 1	51.7 ± 5.5	48.3 ± 4.8	-	-	-
	Layer 2	52.3 ± 4.3	-	45.6 ± 1.2	-	2.1 ± 0.2
B	Layer 1	45.1 ± 4.0	54.9 ± 4.6	-	-	-
	Layer 2	55.8 ± 4.6	-	44.2 ± 0.9	-	-

Figure 2 illustrates the phase composition of the substrate and the coatings formed on it. Characteristic reflections of tungsten carbide and cobalt can be seen on the substrate. In the case of Sample B, the reflections of the deposited coating also appear, but with a much lower intensity than in the case of Sample A. As was also visible in the scanning electron microscope images, the TiN coating is present in a better crystallized form on the surface of Sample A, with characteristic reflections of this being much more intense.

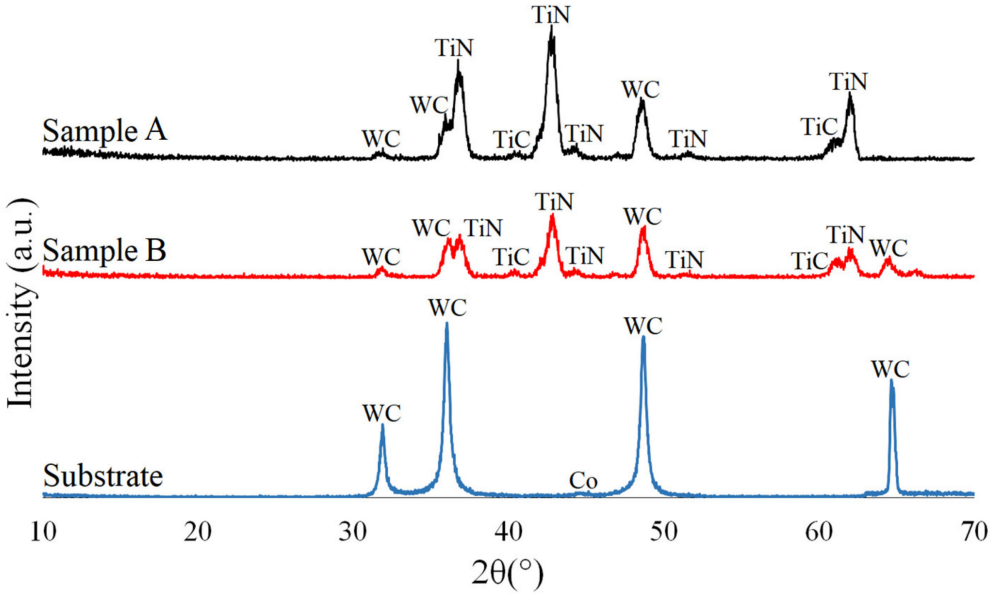


Figure 2. Phase composition of the substrate and the coated samples.

2.2. Methods

Morphology was examined using a FEI/Thermo Fisher Apreo S scanning electron microscope (SEM, Brno, Czech Republic). The SEM observations were conducted under high-vacuum conditions with an accelerating voltage of 20.0 kV. To obtain the best resolution for back-scattered electron imaging, the samples were washed in an ultrasonic bath using ethanol and acetone. To prepare the cross-section, the samples were embedded in epoxy resin (NXMET XF40) and polished. The elemental compositions of the samples were determined using an EDAX Octane Elect Plus Energy Dispersive X-ray Analyzer (Ametek GmbH, Wiesbaden, Germany). The accelerating voltage was 20 kV and the data collection time was 180 s.

The microhardness test was performed on both the coated and uncoated (reference) samples and characterized by the Vickers microhardness (4.903 N, Wolpert 402 MVD, Fritz Müller GmbH, München, Germany) with a 0.2 kgf loading force. The hardness was recorded as an average of five readings for each specimen.

The X-ray diffraction (XRD) analyses of the samples were performed using a Philips PW 3710 diffractometer (PANanalytical B.V., Almelo, Netherlandsmanufacturer, city, state (only for USA and Canada), country). The measurement parameters were as follows: CuK radiation (50 kV, 40 mA), a speed of 0.02 2θ/s, a range of 10 to 70 degrees 2θ, and a curved graphite monochromator. The X'Pert Data Collector software (version 2.0e) was used to collect XRD pattern data. The High Score Plus 5.0 software was used to identify phases and to perform quantitative phase analysis using the Rietveld method. The crystalline phases were identified by comparing the XRD patterns with the 2021 Powder Diffraction Files (PDF-2 2021) from the International Centre of Diffraction Data (ICDD).

The tribological behavior was examined through dry-sliding experiments using an TRB^3 type tribometer (Anton Paar GmbH, Buchs, Switzerland) in a ball-on-disc arrangement. The pin-on-disc tests were carried out in accordance with ASTM G99 [38] and ASTM G133 [39] standards. The coatings were tested against steel (Anton Paar GmbH, Buchs, Switzerland) 100Cr6 steel ball) and zirconia (Fritsch GmbH, Idar-Oberstein, Germany, zirconium oxide grinding ball) balls with diameters of 6 mm and 5 mm, respectively, at 25 °C in ambient air with a relative humidity of 46 ± 3%. The maximum sliding speed and normal load were kept constant at 15.71 cm/s and 20 N, respectively. The coefficient of friction in relation to sliding distance was recorded during the tests. Then, the wear track was cleaned with alcohol to remove loose wear debris, and the wear track was measured

using a profilometer. To compare the wear resistance of the coatings, the wear volume (V_P, mm^3) values were calculated according to the standards above:

$$V_P = (\pi h/6)\,[3D^2/4 + h^2], \quad (1)$$

where h is the height of the removed material from the ball (mm), and D is the diameter of the wear scar on the ball. The height of the material removed can be calculated as follows:

$$h = R - [R^2 - (D^2/4)^{1/2}] \quad (2)$$

where R is the original ball radius (mm).

A modified scratch test was used to investigate the adhesion of the coatings. During the examination, an TRB^3 type tribometer (Anton Paar GmbH, Buchs, Switzerland) was used with a total stroke length of 10 mm and a constant normal force of 5 N. The diamond indentation marks on the surface were evaluated using a scanning electron microscope. Additionally, the surface roughness parameters were determined using a Surtronic S128 (Taylor Hobson GmbH, Leicester, England). A thermal camera (Trotec GmbH, Heinsberg, Germany) with model Trotec XC300 was used to investigate the change in temperature during the tribology test against steel and zirconia balls.

3. Results

3.1. Vickers Hardness Analysis

The microhardness test is a well-established method used to evaluate the mechanical properties of hard CVD coatings. In terms of Vickers hardness, it is a critical property that affects the wear resistance and tool life of cutting tools. In Table 4, the results of the Vickers hardness test are presented for coated and uncoated samples, and it can be seen that the hardness value of the coated sample is significantly higher than that of the uncoated sample. This improvement in hardness is due to the CVD technique, which is aimed at improving the hardness of the coating layer. The increase in hardness from 1895 to more than 2460 demonstrates the effectiveness of the CVD technique in enhancing the mechanical properties of the coating layer. It is also important to note that the hardness values of the coated samples were influenced by the manufacturing conditions, specifically the pressure and temperature, as shown in Table 1. The difference in these conditions resulted in different hardness values between the two samples. So, higher deposition temperatures and pressures lead to harder coatings. This is because higher temperatures and pressures allow for more energetic and aggressive reactions between the precursor gases, leading to denser and more tightly bonded coatings.

Table 4. Vickers microhardness of the coatings and the substrate.

HV 0.2	A	B	WC–Co
AV	2461	2158	1895
SD	327	313	791

3.2. Tribological Analysis of the TiN/TiC Coatings

The effect of sliding time on the coefficient of friction of CVD-coated samples against steel ball and zirconia ball is presented in Figure 3. The values shown on Figure 3 represent the displacement from the starting position of the static counterpart. The measurement was modeled as linearly alternating motion over a total distance of 10 mm. At the 0 mm position ($\mu = 0$) the specimen is at maximum speed and its acceleration is zero, while at the +5 mm (μ value is positive) and −5 mm (μ is negative) positions, the counterpart's speed is zero and its acceleration is maximum. If the coefficient of friction values obtained during the measurement are not symmetrical, it may indicate that the specimen and the counterpart were not properly parallel to each other, the surface of the sample was heterogeneous, or the surface roughness was uneven. The average COF and standard deviation values obtained

during the measurement were indicated in the caption of Figure 3. The friction coefficient charts show that both samples exhibit similar behavior against the steel ball, with a slight initial increase in the friction coefficient attributed to the friction between the surface of the CVD-coated sample and the steel ball. Subsequently, the friction coefficient value stabilizes due to the stick and adhesion of steel on the sample surface, as confirmed by SEM which revealed high concentrations of iron and carbon. The blue line on Figure 3a,c indicates the section where the coefficient of friction value is high ($\mu \approx 1$), and then it becomes constant over time. In the case of Sample A, it took about 20 s (~3 m) to reach the stationary state, while in the case of Sample B, it took 60 s (~10 m) (Figure 3e). This difference is due to the fact that the coating on Sample A, which has well-crystallized, sharp grains, wore down the steel ball faster than the coating on Sample B.

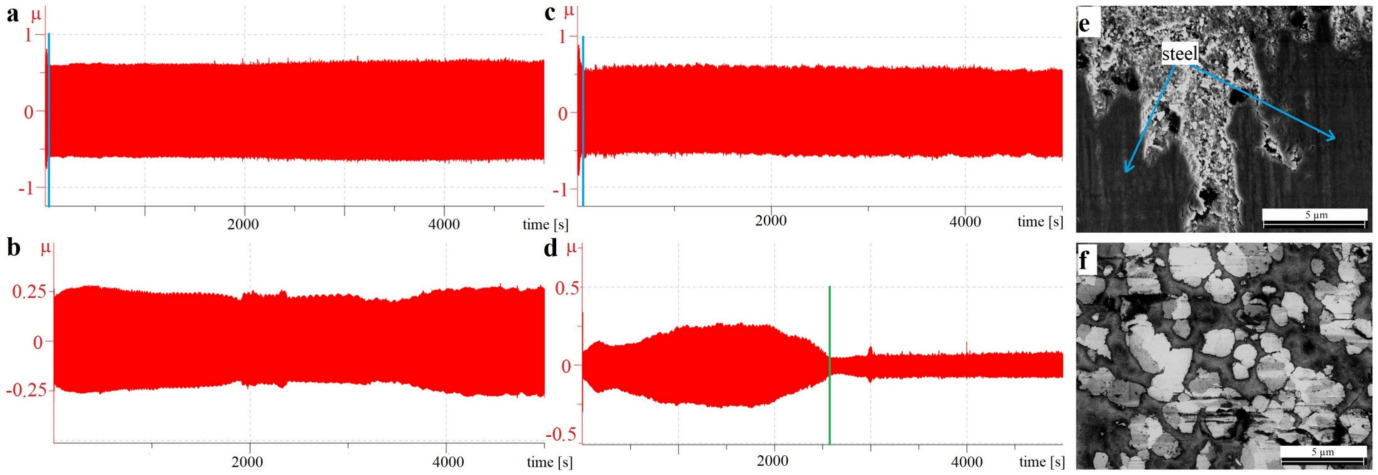
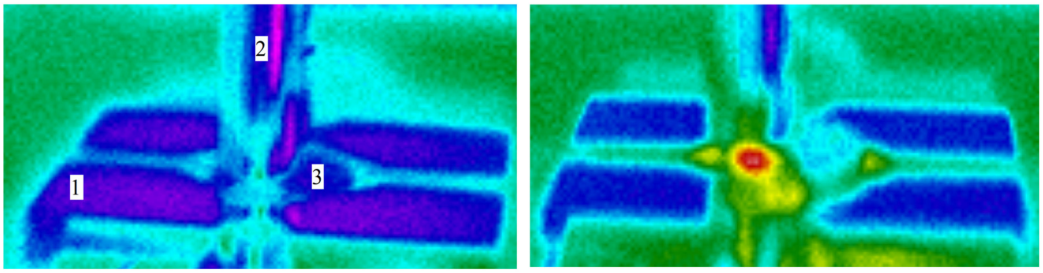


Figure 3. Fluctuation of coefficient of friction values as a function of sliding time (the linear speed of the static counterpart was 0.1571 m/s): (**a**) Sample A against steel ball (μ_{av} = 0.027; sd = 0.509); (**b**) Sample A against ZrO_2 static partner (μ_{av} = 0.002; sd = 0.154); (**c**) Sample B against steel (μ_{av} = 0.010; sd = 0.358); (**d**) Sample B against zirconia (μ_{av} = 0.009; sd = 0.108), and the surface morphology of Sample A after tribological test against steel (**e**), and zirconia (**f**).

The tribological behavior of CVD-coated samples under sliding conditions against the zirconia ball was investigated, and the results were compared to those obtained when using steel balls. The initial observation revealed that the behavior of the friction coefficient changed as a function of sliding time, which was different than when using steel balls. In addition, the coefficient of friction is observed to be lower in the case of zirconia balls, as shown in Figure 3b. However, as the sliding progressed, the friction coefficient slightly increased due to the detached particles during the wear not adhering to the surface as well as in the case of steel, but generating an abrasive effect between the two surfaces and wearing the surface. As shown in Figure 3d, the friction coefficient initially increased, then decreased significantly. This phenomenon is due to poorer adhesion and thickness of the coating in the case of Sample B; therefore, after about 2500 s (~400 m), the TiN coating completely wore off from the surface (marked with a green line on the graph where the coating detached from the surface). During the friction and wear mechanism, the zirconium ball also wore to the same extent, so the measurement continued between surfaces with low surface roughness, resulting in the lowest friction coefficient value in this case ($\mu \approx 0.10$). Figure 3f shows the secondary electron image of the polished surface of Sample B. It can be seen that the coating wore off of the surface, and traces of the polished parts of the WC particles can be observed.

These findings are significant as they provide insight into the influence of the type of ball used on the tribological test of coated CVD samples. The observed decrease in friction coefficient in the case of zirconia balls could be attributed to the differences in the properties of the balls. The slight increase in friction coefficient could be due to the formation of wear lines and surface roughening, which are common phenomena observed during sliding wear tests. The stability of the average values of the friction coefficient after the operation phase suggests that the coated TiN/TiC CVD samples were able to withstand the sliding conditions without significant degradation.

Also, its noteworthy that the heat generated from the frictional interaction between the surface of the CVD-coated samples and the zirconia ball was significantly lower than that produced during testing with the steel ball, as shown in Figure 4 which illustrates the temperature profiles of the CVD-coated samples captured via an infrared camera during the dry sliding test. This finding highlights the advantages of using a zirconia ball over a steel ball, as it generates lower heat during dry sliding tests.



(**a**) (**b**)

Figure 4. Temperature profiles of CVD-coated specimens during dry sliding by Infrared camera: (**a**) against zirconia ball, (**b**) against steel ball; where number 1 denotes the sample holder, number 2 and number 3 shows the static and the sample, respectively.

Table 5 summarizes the results of dry sliding tests performed on CVD-coated samples using steel and zirconia balls, after sliding for a distance of 500 m. The results indicate that the wear values of the steel ball for Sample A and Sample B are approximately 6.08×10^7 μm^3 and 5.05×10^7 μm^3, respectively. In contrast, the wear volumes when using zirconia balls for samples are significantly smaller, at 1.55×10^5 μm^3 and 1.85×10^5 μm^3, respectively. This significant reduction in wear-volume loss between the results of zirconia and steel balls can be attributed to the high hardness of zirconia, which exceeds that of steel. Additionally, the SEM analysis indicated that zirconia balls do not adhere to the surface of the coated sample, resulting in less friction and heat generated during the motion of the test ball and sample surface.

Table 5. Volume loss of the steel and zirconia balls after sliding test.

Sample	D (mm)	h (mm)	V_P (μm^3)
Sample A against steel	1.648	0.057	6.08×10^7
Sample A against ZrO_2	0.397	0.003	1.85×10^5
Sample B against steel	1.572	0.052	5.05×10^7
Sample B against ZrO_2	0.363	0.003	1.55×10^5

It is worth noting that the variation in wear-volume loss values for coated samples is due to multiple reasons, with the most significant being the difference in preparation parameters, particularly pressure and temperature, as shown in Table 1. The hardness value of Sample A is 14% higher than that of Sample B, as shown in Table 4, and the thickness of the coating layers in Sample A is approximately 68% greater than that of Sample B. All of these factors contributed to reducing the wear rate of Sample B, which is approximately 16% less than that of Sample A against the steel ball and 17% less against the zirconia ball. These

results provide valuable insights into the tribological behavior of coated CVD samples. Moreover, the use of zirconia balls in the tribological testing of CVD-coated samples may be more appropriate, as it provides more accurate and realistic results. The high hardness of zirconia makes it less prone to wear and tear, and it does not adhere to the surface of the coated sample, resulting in less friction and heat generation during the sliding process. Therefore, the use of zirconia balls can improve the accuracy and reliability of tribological testing results for CVD-coated samples [40].

3.3. Surface Morphology and Roughness Analysis

The current study investigated the tribological behavior of CVD-coated samples using both steel and zirconia balls, with the microstructural and compositional analysis conducted using EDS. Figure 5 shows the EDS line scan results of the coated samples after a tribological test at a sliding distance of 500 m, where the y-axis indicates the atomic percentage distribution and the x-axis shows the distance (the line analysis was performed along the red line shown in Figures 5 and 6, using backscattered electron imaging). As previously shown, during tests with a steel counterpart, the steel adhered to the coating surface, so before the EDS tests it was removed with an 18 vol.% hydrochloric acid solution, and before the test, each sample was washed in an ultrasonic bath with ethanol.

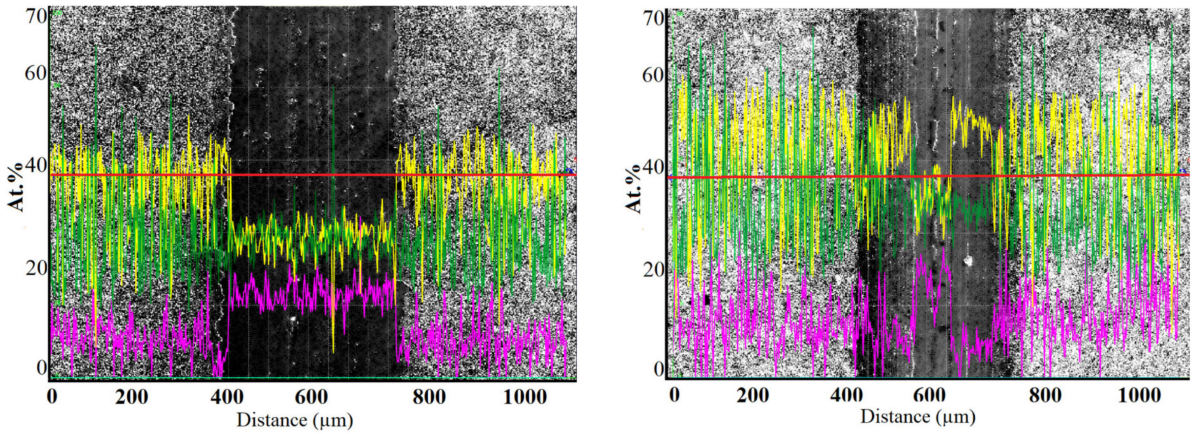


Figure 5. Distribution of the elements among the wear track: (**a**) Sample A against steel; (**b**) Sample A against zirconia, where Ti is marked in yellow, N in green, and C in pink.

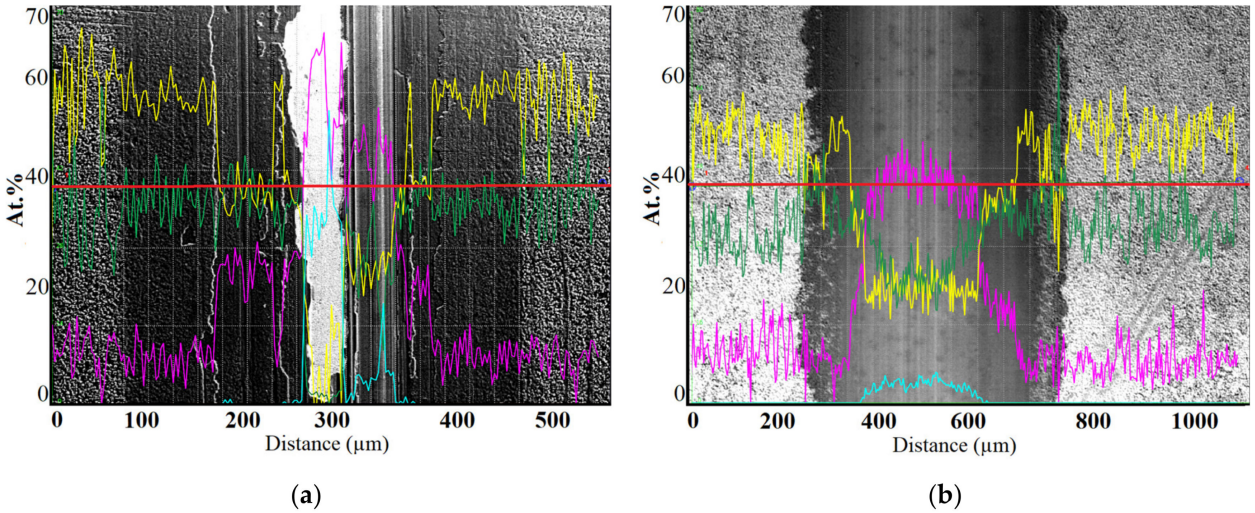


Figure 6. Elemental distribution after sliding test: (**a**) Sample B against steel; (**b**) Sample B against ZrO_2, where Ti is marked in yellow, N in green, C in pink, and W in blue.

The line scan analysis of Sample A after using steel and zirconia in Figure 5a shows that the coating area contains C, Ti and N, represented by the colors pink, yellow, and green, respectively. The wear traces start from 400 µm and continue to 800 µm, with the coating still present and no trace of the substrate (W) detected. The figure clearly shows that the amount of Ti and N decreased along the wear track, while the C content increased. This indicates that the top TiN layer wore off during the 500 m tribotest. A similar phenomenon was observed during the wear test of Sample A with zirconium oxide, although in this case only a narrow range of the top layer was worn off, as shown in Figure 5b around the 600 µm distance. The results demonstrate that the wear resistance of Sample A is excellent against both steel and zirconia.

The wear characteristics of Sample B were investigated against steel and zirconia balls, as shown in Figure 6a,b. During the tribological test with the steel counterpart, in the case of Sample B, both the TiN and TiC layers completely detached from the substrate surface in the vicinity of 300 µm sliding distance. The flake-like detachment indicates that the adhesion between the coated layer and the deposited steel was presumably greater than that between the substrate and the TiC coating. Along the wear track, the W atomic percentage in the substrate was nearly 50%.

In the tribological test with the zirconium counterpart, the TiN layer of the Sample B almost completely detached, while the TiC layer partially detached from the surface. This phenomenon was also supported by changes in the friction coefficient (Figure 3b,f). At a sliding distance of 400–600 µm, the blue color indicates the presence of the substrate.

As the TiC coating was not removed by the 500 m tribological test in the case of sample A, a 1550 m test was also conducted with a zirconium static counterpart. The changes in volume loss values measured after the 50 m, 150 m, 350 m, 750 m, and 1550 m wear tests are illustrated in Figure 7. The y-axis on the graph shows the natural logarithm of the volume loss, while the x-axis shows the natural logarithm of the sliding distance. It can be seen from the results that a significant amount of zirconium was detached from the contact surface of the ball after the 50 m wear test. This phenomenon can be attributed to the TiN layer containing numerous small crystals with sharp edges in this case. The wear amount sharply decreases up to 750 m, and then slightly increases between 750 and 1550 m. This phenomenon can be attributed to particles that detached from the contact surface of the static zirconia counterpart over a distance 800 m between the last two measurement points, which exerted an abrasive effect. As a result of these particles detaching, there was a slight increase in volume loss. In this case, the partial detachment of the TiC coating may have already started, and the abrasive wear processes of the particles present on the contact surface further wore down the zirconium ball.

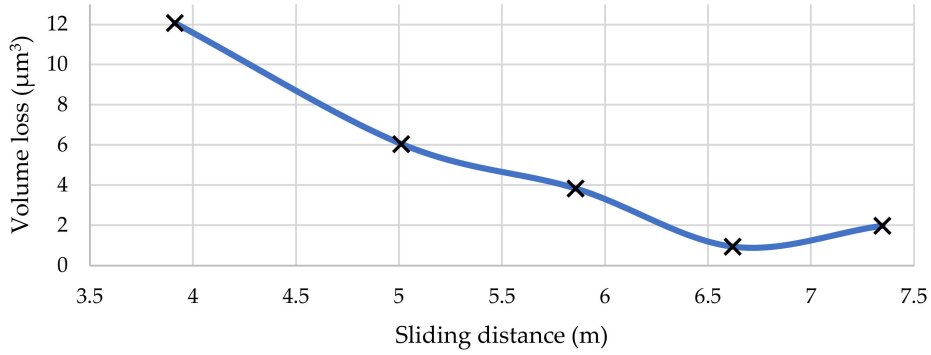


Figure 7. Wear rate of the zirconia ball as a function of sliding distance.

After the 1550 m wear test, the results of the line scan analysis are shown in Figure 8. The wear track is visible between 200 µm and 1000 µm. The TiN and TiC layers were completely removed from the surface in the area of 800 µm, which is indicated by the presence of the blue color representing W.

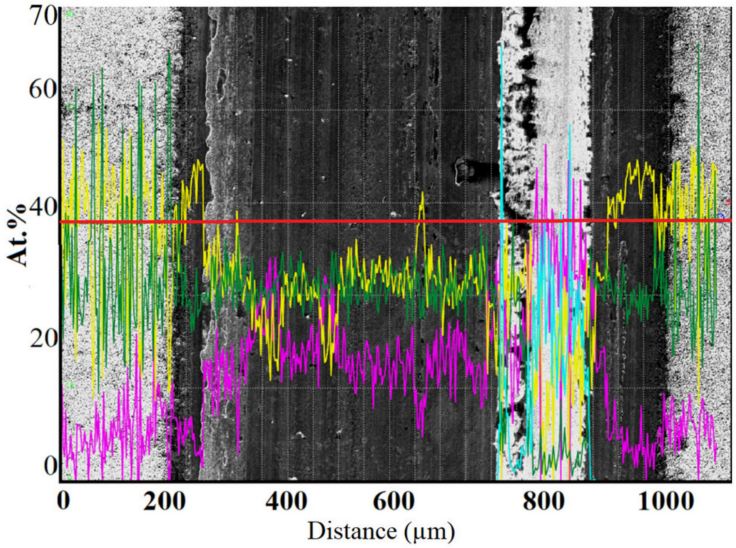


Figure 8. Elemental distribution of the wear track of Sample A after 1550 m sliding test, where Ti is marked in yellow, N in green, C in pink, and W in blue.

Surface roughness is a significant factor that can affect the tribological properties of CVD coatings, including their wear resistance and friction coefficient. The results presented in Table 6 provide important insights into the impact of using steel and zirconia balls in tribological testing of CVD-coated samples. In the case of Samples A and B, the average surface roughness value increased in each case following the wear tests. As for sample A, a slight increase was observed after the wear tests, especially in relation to the tests conducted with the zirconium counterpart. This phenomenon suggests that the small, hard particles detached from the zirconium dug deeper grooves into the surface, despite the TiC coating not detaching from the substrate. A similar phenomenon was observed in the case of Sample B, with the difference that, following the tests conducted with the steel counterpart, the Ra and Rz values were higher, which can be attributed to the coating peeling off in a scale-like manner. The Rp/Rz value of each starting sample was less than 0.5, which indicates a tribologically favorable surface. This value increased as a result of the wear tests, meaning that the surface became more rough and defined by rough peaks.

Table 6. Changes in surface roughness values following wear tests.

Sample	Ra [μm]	Rz [μm]	Rp [μm]	Rp/Rz
Sample A	0.19	1.74	0.84	0.48
Sample B	0.15	1.65	0.81	0.49
Sample A against steel	0.29	2.41	1.23	0.51
Sample A against ZrO_2	0.42	2.58	1.37	0.53
Sample B against steel	0.40	2.55	1.28	0.50
Sample B against ZrO_2	0.35	3.06	1.57	0.51
Sample A against ZrO_2 after 1550 m	0.73	4.57	2.39	0.52

Furthermore, Table 6 demonstrates that the surface roughness of Sample A against zirconia increased to 0.73 after a sliding distance of 1550 m. These results indicate that there is a positive correlation between sliding distance and surface roughness, suggesting that TiN and TiC coatings did not necessarily delaminate from the surface in a homogeneous manner.

3.4. Adhesion Test of the Coatings

In the scratch test, a non-standard method was used to investigate the adhesion of the coatings. During the measurement, the normal compressive force was kept constant at 5 N, and the total scratch length was 10 mm. The evaluation of the results was based on SEM micrographs (Figure 9).

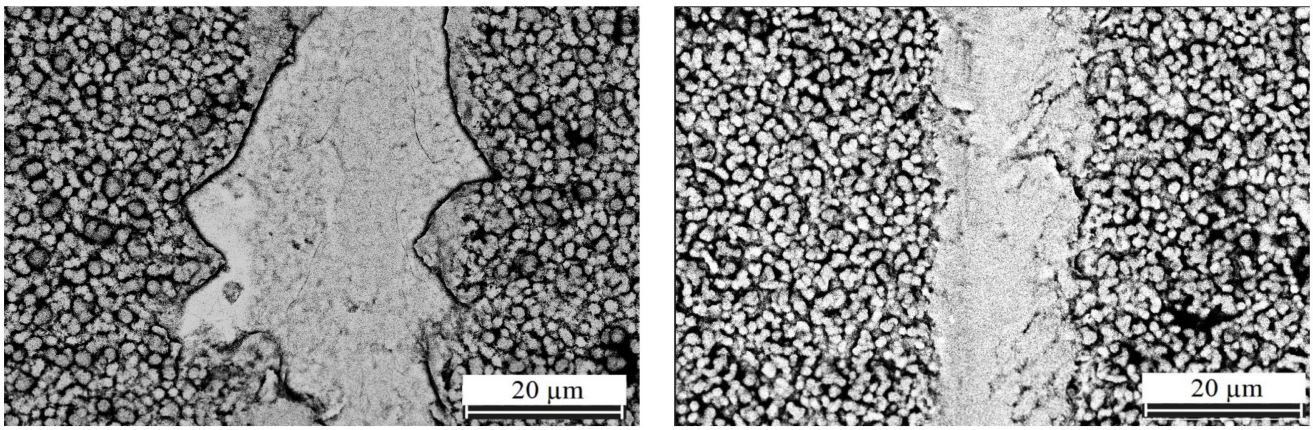


Figure 9. Pressure channel formed after scratch test: (**a**) Sample A; (**b**) Sample B.

For Sample A, the coating chipped along the scratch line, and irregular edges were observed around the pressure channel. However, for Sample B, such significant material removals were not observed. The coating did not separate from the surface, but rather smeared. Based on previous SEM and XRD results, it was observed that the coating on Sample A was present in a better crystallized form, with regular small crystals forming the coating. The results obtained from the scratch test indicate that the coating is more rigid, more brittle, and has lower fracture toughness. Kupstov et al. [21] observed a similar phenomenon during the standard scratch test of TiCN-based coatings. TiAlSiCN and TiCrSiCN layers produced by SHS method exhibited similar rigid and brittle behavior. Despite the fact that during the scratch test, the coating on Sample A was removed to a greater extent, the sample with better-crystallized, thicker coating exhibited better tribological properties.

4. Conclusions

During the examination, TiN and TiC coatings produced with different manufacturing parameters were tested for tribological wear resistance using steel and zirconium counterparts. Based on the tests, it can be concluded that it is advisable to use a zirconium counterpart even for coatings with different layer thicknesses and hardnesses in the pin-on-disc method. The coefficient of friction test proved that steel adheres to the surface during the first 20–60 s of the test, making it unsuitable for wear tests of CVD coatings.

Using a zirconium oxide static counterpart, the wear and friction behavior of TiN/TiC coatings can be excellently tracked in linear tribological model experiments. By examining the fluctuation in coefficient of friction values, it is possible to monitor when multilayer coatings start to peel off. When a steel counterpart is used, a stationary state is reached after a certain period of time. The tribological investigation of zirconia-based counterparts and CVD-coated specimens can provide valuable results for processing ceramic products, as it is important in this case that the TiN and TiC layers are present in a regular, well-crystalized form with the appropriate thickness. Another important consideration when processing similar material systems is the heating of components, which can also be overcome by using zirconium. Surface roughness and scratch test examinations have demonstrated that, despite the rigid and brittle nature of TiN/TiC layer, it exhibits advantageous tribological properties.

Author Contributions: Conceptualization, M.J. and O.I.A.; methodology, M.J.; validation, M.J., O.I.A. and T.K.; formal analysis, M.J. and O.I.A.; investigation, O.I.A.; data curation, M.J. and T.K.; writing—original draft preparation, O.I.A.; writing—review and editing, M.J.; visualization, O.I.A. and M.J.; supervision, I.G.G., T.K and J.T. All authors have read and agreed to the published version of the manuscript.

Funding: This work was supported by the TKP2020-NKA-10 project financed under the 2020-4.1.1-TKP2020 Thematic Excellence Programme by the National Research, Development and Innovation Fund of Hungary.

Institutional Review Board Statement: Not applicable.

Informed Consent Statement: Not applicable.

Data Availability Statement: All data that support the findings of this study are included within the article.

Acknowledgments: The project with code 2019-1.1.1-PIACI-KFI-2019-00506 was implemented with the support of the Ministry of Innovation and Technology, through the National Research Development and Innovation Fund. The project was funded under the Market-driven Research and Innovation Projects Support Programme.

Conflicts of Interest: The authors declare no conflict of interest.

References

1. Sharma, R.; Pradhan, S.; Bathe, R.N. Design and Fabrication of Spiral Triangular Micro Texture on Chemical Vapor Deposition Coated Cutting Insert Using Femtosecond Laser Machine. *Mater. Today Proc.* **2020**, *28*, 1439–1444. [CrossRef]
2. Martin, P.M. *Handbook of Deposition Technologies for Films and Coatings: Science, Applications and Technology*; William Andrew: Norwich, NY, USA, 2009; ISBN 978-0-8155-2032-0.
3. Gyurika, I.G.; Ali, O.I.; Jakab, M. Determination of Research Guidelines and Establishing of a Test Framework for the Development of New CVD Coating Formulations and New Approach Coating Equipment. In *Proceedings of the Smart Technologies in Urban Engineering*; Arsenyeva, O., Romanova, T., Sukhonos, M., Tsegelnyk, Y., Eds.; Springer International Publishing: Cham, Switzerland, 2022; pp. 420–431.
4. Jones, A.C.; Hitchman, M.L. *Chemical Vapour Deposition: Precursors. Processes and Applications*; Royal Society of Chemistry: London, UK, 2009; ISBN 978-0-85404-465-8.
5. Aper, T.M.; Yam, F.K.; Beh, K.P. Influence of Temperature and Nickel Catalyst on the Structural and Optical Properties of Indium Oxide Nanostructured Films Synthesized by Chemical Vapor Deposition Technique. *Mater. Sci. Semicond. Process.* **2021**, *132*, 105925. [CrossRef]
6. Bhaduri, B. Synthesis of Cu Catalyzed Chemical Vapor Deposition Grown Cu-CNFs on Less Porous Graphite Powder. *Mater. Lett.* **2021**, *305*, 130828. [CrossRef]
7. Uhlmann, E.; Schröter, D. Process Behaviour of Micro-Textured CVD Diamond Thick Film Cutting Tools during Turning of Ti-6Al-4V. *Procedia CIRP* **2020**, *87*, 25–30. [CrossRef]
8. Ma, Z.; Song, J.; Fan, H.; Hu, T.; Hu, L. Preparation and Study on Fretting Tribological Behavior of Composite Lubrication Structure on the Titanium Alloy Surface. *Coatings* **2022**, *12*, 332. [CrossRef]
9. Shen, T.; Zhu, L.; Liu, Z. Effect of Micro-Blasting on the Tribological Properties of TiN/MT-TiCN/Al_2O_3/TiCNO Coatings Deposited by CVD. *Int. J. Refract. Met. Hard Mater.* **2020**, *88*, 105205. [CrossRef]
10. Bai, H.; Zhong, L.; Kang, L.; Liu, J.; Zhuang, W.; Lv, Z.; Xu, Y. A Review on Wear-Resistant Coating with High Hardness and High Toughness on the Surface of Titanium Alloy. *J. Alloys Compd.* **2021**, *882*, 160645. [CrossRef]
11. Jadhav, P.M.; Reddy, N.S.K. Analysis of Novel Nano-Composite Coating for Varied Combinations of YSZ1–x–y. TiNx. SiNy. *Tribol. Trans.* **2020**, *63*, 683–703. [CrossRef]
12. Ruppi, S.; Larsson, A. Deposition. Microstructure. and Properties of Nanocrystalline Ti(C.O.N) Coatings. *J. Vac. Sci. Technol. Vac. Surf. Films* **2003**, *21*, 66–75. [CrossRef]
13. Moura, C.; Cunha, L.; Chappé, J.M.; Vaz, F. Study on the Thermal Stability of Ti(C.O.N) Decorative Coatings. *Plasma Process. Polym.* **2009**, *6*, S755–S759. [CrossRef]
14. Zhu, L.; Zhang, Y.; Hu, T.; Leicht, P.; Liu, Y. Oxidation resistance and thermal stability of Ti(C.N) and Ti(C.N.O) coatings deposited by chemical vapor deposition. *Int. J. Refract. Met. Hard Mater.* **2016**, *54*, 295–303. [CrossRef]
15. Hsieh, J.H.; Wu, W.; Li, C.; Yu, C.H.; Tan, B.H. Deposition and characterization of Ti(C.N.O) coatings by unbalanced magnetron sputtering. *Surf. Coat. Technol.* **2003**, *163–164*, 233–237. [CrossRef]

16. Kenzhegulov, A.; Mamaeva, A.; Panichkin, A.; Alibekov, Z.; Kshibekova, B.; Bakhytuly, N.; Wieleba, W. Comparative Study of Tribological and Corrosion Characteristics of TiCN. TiCrCN. and TiZrCN Coatings. *Coatings* **2022**, *12*, 564. [CrossRef]
17. Zhu, M.; Achache, S.; Boulet, P.; Virfeu, A.; Pierson, J.-F.; Sanchette, F. Effects of Deposition Parameters on the Microstructure and Mechanical Properties of Ti(C.N) Produced by Moderate Temperature Chemical Vapor Deposition (MT-CVD) on Cemented Carbides. *Vacuum* **2022**, *195*, 110650. [CrossRef]
18. Czettl, C.; Mitterer, C.; Mühle, U.; Rafaja, D.; Puchner, S.; Hutter, H.; Penoy, M.; Michotte, C.; Kathrein, M. CO Addition in Low-Pressure Chemical Vapour Deposition of Medium-Temperature TiCxN1-x Based Hard Coatings. *Surf. Coat. Technol.* **2011**, *206*, 1691–1697. [CrossRef]
19. Azadi, M.; Rouhagdam, S.A.; Ahangarani, S.; Mofidi, H.H.; Valiei, M. Mechanical behaviour and properties of TiN/TiC coating using PACVD. *Adv. Mater. Res.* **2014**, *829*, 476–481. [CrossRef]
20. Günen, A.; Soylu, B.; Karakas, Ö. Titanium carbide coating to improve surface characteristic, wear and corrosion resistance of spheroidal graphite cast irons. *Surf. Coat. Technol.* **2022**, *437*, 128280. [CrossRef]
21. Kupstov, A.K.; Kiryukhantsev-Korneev, P.V.; Sheveyko, A.N.; Shtanksy, D.V. Comparative study of electrochemical and impact wear behaviour of TiCN, TiSiCN, TiCrSiCN, and TiAlSiCN coatings. *Surf. Coat. Technol.* **2013**, *216*, 273–281. [CrossRef]
22. Lengauer, W. Transition Metal Carbides. Nitrides. and Carbonitrides. In *Handbook of Ceramic Hard Materials*; John Wiley & Sons. Ltd.: Hoboken, NJ, USA, 2000; pp. 202–252. ISBN 978-3-527-61821-7.
23. Larsson, A.; Ruppi, S. Microstructure and Properties of Ti(C.N) Coatings Produced by Moderate Temperature Chemical Vapour Deposition. *Thin Solid Films* **2002**, *402*, 203–210. [CrossRef]
24. Wagner, J.; Mitterer, C.; Penoy, M.; Michotte, C.; Wallgram, W.; Kathrein, M. Structure and Properties of CVD TiCxN1-x Coatings. In *16th International Plansee Seminar*; Kneringer, G., Rödhammer, P., Wildner, H., Eds.; Plansee AG: Reutte, Austria, 2005; pp. 917–931.
25. Hutchings, I.; Shipway, P. *Tribology: Friction and Wear of Engineering Materials*, 2nd ed.; Butterworth-Heinemann: Cambridge, MA, USA, 2017; ISBN 978-0-08-100910-9.
26. Holmberg, K.; Matthews, A. *Coatings Tribology: Properties. Mechanisms. Techniques and Applications in Surface Engineering*, 2nd ed.; Elsevier Science: Amsterdam, The Netherlands; Boston, MA, USA, 2009; ISBN 978-0-444-52750-9.
27. Zhong, Z.Q.; Zhang, L.; Zhou, L.; Qiu, L.-C.; Shi, H.-D.; Yang, M.-L.; Zhu, J.-F. Cutting Performances and the Related Characteristics of CVD Coated Hardmetal Inserts Changed by Post-Treatments. *Int. J. Refract. Met. Hard Mater.* **2018**, *70*, 162–168. [CrossRef]
28. Karaoglanli, A.C.; Caliskan, H.; Gok, M.S.; Erdogan, A.; Turk, A. A Comparative Study of the Microabrasion Wear Behavior of CoNiCrAlY Coatings Fabricated by APS. HVOF. and CGDS Techniques. *Tribol. Trans.* **2014**, *57*, 11–17. [CrossRef]
29. Çalışkan, H.; Kurbanoğlu, C.; Panjan, P.; Čekada, M.; Kramar, D. Wear Behavior and Cutting Performance of Nanostructured Hard Coatings on Cemented Carbide Cutting Tools in Hard Milling. *Tribol. Int.* **2013**, *62*, 215–222. [CrossRef]
30. Hooper, R.M.; Morgan, J.E. Wear processes in the diamond grinding of zirconia ceramics. *Wear* **1989**, *130*, 353–356. [CrossRef]
31. Kim, H.; Kim, C.Y.; Kim, D.W.; Lee, I.S.; Lee, G.H.; Park, J.C.; Lee, S.J.; Lee, K.Y. Wear Performance of Self-Mating Contact Pairs of TiN and TiAlN Coatings on Orthopedic Grade Ti-6Al-4V. *Biomed. Mater. Bristol Engl.* **2010**, *5*, 044108. [CrossRef] [PubMed]
32. Aihua, L.; Jianxin, D.; Haibing, C.; Yangyang, C.; Jun, Z. Friction and wear properties of TiN. TiAlN. AlTiN and CrAlN PVD nitride coatings. *Int. J. Refract. Met. Hard Mater.* **2012**, *31*, 82–88. [CrossRef]
33. You, Q.; Xiong, J.; Li, H.; Guo, Z.; Fang, D.; Gou, S. Structure and mechanical behavior evaluation of CVD multilayer coatings deposited on Ti(C.N)-based cermets. *Ceram. Int.* **2022**, *48*, 13250–13259. [CrossRef]
34. You, Q.; Xiong, J.; Li, H.; Guo, Z.; Huo, Y. Study on the Microstructure and High Temperature Friction and Wear Characteristics of Three CVD Coated Cermets. *Int. J. Refract. Met. Hard Mater.* **2021**, *96*, 105495. [CrossRef]
35. Hsieh, J.H.; Tan, A.L.K.; Zeng, X.T. Oxidation and Wear Behaviors of Ti-Based Thin Films. *Surf. Coat. Technol.* **2006**, *201*, 4094–4098. [CrossRef]
36. Yoon, S.Y.; Kim, J.K.; Kim, K.H. A comparative study on tribological behavior of TiN and TiAlN coatings prepared by arc ion plating technique. *Surf. Coat. Technol.* **2002**, *161*, 237–242. [CrossRef]
37. Dekker, J.P.; van der Put, P.J.; Veringa, H.J.; Schoonman, J. A Kinetic Study of Titanium Nitride Chemical Vapor Deposition Using Nitrogen. Hydrogen. and Titanium Tetrachloride. *J. Electrochem. Soc.* **1994**, *141*, 787. [CrossRef]
38. *ASTM G99-05*; Standard Test Method for Wear Testing with a Pin-on-Disk Apparatus. ASTM International: West Conshohocken, PA, USA, 2010. [CrossRef]
39. *ASTM G133-05*; Standard Test Method for Linearly Reciprocating Ball-on-Flat Sliding Wear. ASTM International: West Conshohocken, PA, USA, 2010. [CrossRef]
40. Krbata, M.; Eckert, M.; Bartosova, L.; Barenyi, I.; Majerik, J.; Mikuš, P.; Rendkova, P. Dry Sliding Friction of Tool Steels and Their Comparison of Wear in Contact with ZrO_2 and $X46Cr_{13}$. *Materials* **2020**, *13*, 2359. [CrossRef] [PubMed]

Disclaimer/Publisher's Note: The statements, opinions and data contained in all publications are solely those of the individual author(s) and contributor(s) and not of MDPI and/or the editor(s). MDPI and/or the editor(s) disclaim responsibility for any injury to people or property resulting from any ideas, methods, instructions or products referred to in the content.